

Particle size reduction: A way to enhanced dielectric properties of magnetocapacitive $\text{La}_{2/3}\text{Ca}_{1/3}\text{MnO}_3$

S. Yáñez-Vilar,¹ J. Mira,^{2,a)} M. Sánchez-Andújar,¹ S. Castro-García,¹ A. Fondado,² J. Rivas,² and M. A. Señarís-Rodríguez¹

¹Dpto. Química Fundamental, Universidade da Coruña, 15071 A Coruña, Spain

²Dpto. Física Aplicada, Universidade de Santiago de Compostela, 15782 Santiago de Compostela, Spain

(Received 14 January 2010; accepted 15 March 2010; published online 21 April 2010)

We report the optimization of the dielectric properties of $\text{La}_{2/3}\text{Ca}_{1/3}\text{MnO}_3$. This is achieved by synthesizing this material with small particle size, strategy that reduces the conductivity of the sample and its dielectric losses, while retaining a reasonably high dielectric permittivity and a good magnetocapacitive response. In order to further improve the properties of these nanoparticles, we have also prepared core-shell composites $\text{La}_{2/3}\text{Ca}_{1/3}\text{MnO}_3 @ \text{SiO}_2$ but in this case the magnetocapacitive effect is strongly reduced. © 2010 American Institute of Physics.

[doi:10.1063/1.3394004]

The variation in the capacitance of a material under an applied magnetic field (magnetocapacitance) is a property as useful as difficult to achieve. The reason is that multiferroics (materials with coexistence and coupling of magnetically and electrically ordered phases) are a rare gift of nature because of the contraindication of magnetism and ferroelectricity.^{1,2} Among the different ways to overcome this limitation, one is to focus on compounds with non-conventional mechanisms for ferroelectric and/or magnetic ordering such as: the so-called “geometric” ferroelectrics,³ materials combining A-site (lone pair) ferroelectricity with B-site magnetic order⁴ or materials where electrical polarization emerges due to the magnetic order.⁵ In this latter case and in order to obtain the ferroelectric state, the magnetic structure must break the inversion symmetry, a condition observed in noncollinear magnetic phases, such as those with spiral or helicoidal structures. A different approach is to focus on composite materials which combine a magnetically ordered phase with another that shows ferroelectric and piezoelectric properties, and their coupling via strain gives rise to a magnetoelectric effect.⁶

Yet there is another relatively less explored route to obtain a magnetocapacitive material: by the creation of heterogeneous materials made up of insulating and metallic ferromagnetic regions that simultaneously show magnetoresistance and space-charge or interfacial polarization. It is worth mentioning that such type of polarization, that arises at the interface between the phases of different conductivities, is in fact the basis for the fabrication of “non-natural” dielectric systems like cermets.⁷

We have recently demonstrated that this kind of strategy can be “naturally” implemented in materials with electronic phase separation, as the well-known magnetoresistive manganite $\text{La}_{2/3}\text{Ca}_{1/3}\text{MnO}_3$ in which a ferromagnetic metallic phase coexists with an insulating nonmagnetic one,⁸ and in which we have found a large magnetocapacitive response at room temperature and under relatively low magnetic fields.⁹ In this compound, and as also rationalized by Catalan¹⁰ using the Maxwell–Wagner capacitor model, such magnetocapaci-

tance is possible without the need of magnetoelectric coupling. This occurs only by the combination of a variable landscape of phase separation under the magnetic field (that gives rise to the magnetoresistive effect) and the Maxwell–Wagner effect. Moreover, from the theoretical work by Parish and Littlewood,¹¹ it was shown that even magnetism is not a necessary condition for a magnetocapacitance to appear.

Coming back to the case of the magnetocapacitive response of the manganite $\text{La}_{2/3}\text{Ca}_{1/3}\text{MnO}_3$, two major facts are defining the dielectric figures of this effect: the heterogeneity of the sample, necessary for the appearance of interfacial polarization, and the conductivity of the material, which is a drawback for the practical use of this system. We have tried to act directly on them in order to improve the magnetocapacitive figures obtained in bulk $\text{La}_{2/3}\text{Ca}_{1/3}\text{MnO}_3$.

For this purpose we have used two strategies: (a) we have reduced the particle size of the polycrystalline material with the intention of creating additional artificial boundaries that reinforce the already existing natural ones due both to the polycrystalline nature of the sample and to its phase-segregated nature. By this means we try to simultaneously enhance the interfacial polarization and to reduce the sample’s conductivity; (b) once we have obtained the particles of reduced size, we have tried to further reduce their conductivity by coating them with insulating shells of SiO_2 of different thickness.

In this paper we present the obtained results, that show that the magnetocapacitive properties of $\text{La}_{2/3}\text{Ca}_{1/3}\text{MnO}_3$ can be improved this way. The $\text{La}_{2/3}\text{Ca}_{1/3}\text{MnO}_3$ nanoparticles were synthesized by the sol-gel method using La_2O_3 (Aldrich, 99.99%), CaCO_3 (Panreac, 98.5%), and $\text{Mn}(\text{NO}_3)_2 \cdot 5\text{H}_2\text{O}$ (Aldrich, 98%) as starting reagents and urea (Aldrich, 98%) as the gelification agent and using a previously described procedure¹² with a final heating treatment at 700 °C/3 h.

The core-shell composites were prepared by an adaptation of the Stöber method.¹³ For this purpose 50 mg of the $\text{La}_{0.67}\text{Ca}_{0.33}\text{MnO}_3$ particles that constitute the “core” of the composite were dispersed into a solution of propanol (Panreac, 99.5%) containing 2 M of distilled water, whose pH was adjusted to 8–10 with a solution 0.45 M of aqueous

^{a)}Author to whom correspondence should be addressed. Electronic mail: jorge.mira@usc.es.

ammonia (Panreac, 30%). The suspension was subjected to ultrasonic agitation for a hour and subsequently heated to 40 °C. Then, different concentrations of tetraethyl orthosilane (TEOS) (Aldrich, 99.99%), 3×10^{-4} and 4×10^{-4} M were added, while vigorous agitation of the suspension was maintained. The resulting dispersion was allowed to stand for 24 h with vigorous agitation, since the active silica polymerizes onto the mixed oxide surface. The resulting coated material was isolated by centrifugation at ~ 5000 rpm/30', washed with water and then dried.

The obtained materials were studied by x-ray powder diffraction (XRPD) in a Siemens D-5000 diffractometer at room temperature and using $\text{Cu(K}\alpha\text{)}=1.5418$ Å radiation. The XRPD pattern of the $\text{La}_{2/3}\text{Ca}_{1/3}\text{MnO}_3$ base material confirms the purity of the obtained sample and the absence of secondary impurity phases. As for the XRPD pattern of the $\text{La}_{2/3}\text{Ca}_{1/3}\text{MnO}_3 @ \text{SiO}_2$ core-shell composites, they only contains the peaks of the $\text{La}_{2/3}\text{Ca}_{1/3}\text{MnO}_3$ phase, indicating that this is the only crystalline phase present and that SiO_2 must be in an amorphous state.

The granulometry of the samples was tested by transmission electron microscopy in a JEOL 1010 microscope operating at 100 kV. These studies show that the polycrystalline $\text{La}_{2/3}\text{Ca}_{1/3}\text{MnO}_3$ sample consists of homogeneous nanoparticles with average diameter $\phi \sim 100$ nm. After the reaction with TEOS, the entire surface of the nanoparticles gets coated with an uniform SiO_2 shell of approximately 3 and 5 nm of thickness, leading the formation of the $\text{La}_{2/3}\text{Ca}_{1/3}\text{MnO}_3 @ \text{SiO}_2$ core-shell composite.

The complex dielectric permittivity was measured with a parallel-plate capacitor coupled to a precision LCR meter Agilent 4284 A, capable to measure in frequency range from 20 Hz to 1 MHz. The capacitor was mounted in an aluminum box refrigerated with liquid nitrogen, and incorporating a mechanism to control the temperature up to 350 K. The pelletized samples (average size: 0.20–0.30 cm²) were prepared to fit in the capacitor, and gold was sputtered on their surfaces to ensure good electrical contact with the electrodes. Impedance complex plane plots were analyzed using the LEVM program.¹⁴

Figures 1(a) and 1(b) shows the variation in the dielectric constant, ϵ'_r , versus both frequency and temperature for the three samples studied (uncoated $\phi \sim 100$ nm particles, and the same particles with shells of 3 and 5 nm) and its comparison with the data of Ref. 9. With the diminution of the particle size, ϵ'_r decreases due to the reduction in conductivity, shown in Fig. 2(a). In fact, further reductions in conductivity by coating the particles with SiO_2 lead to smaller dielectric constants. From the practical point of view, the overall effect is positive, as the loss tangent falls following this strategy, as seen in Fig. 2(b). Therefore, this reduction in the conductivity of the compound works: it allows us to decrease the loss tangent while maintaining a reasonably high ϵ'_r . If the observed tendency continued for higher frequencies ($\tan \delta$ decreases with frequency more than ϵ'_r does) these materials could be interesting for application in the microwave range.

When we study the influence of an external magnetic field on the dielectric properties we observe that the magnetocapacitive response is also affected by the different preparation of the samples: whereas in the bulk material for 0.5 T at 280 K it is of 35% in all the frequency range measured, for

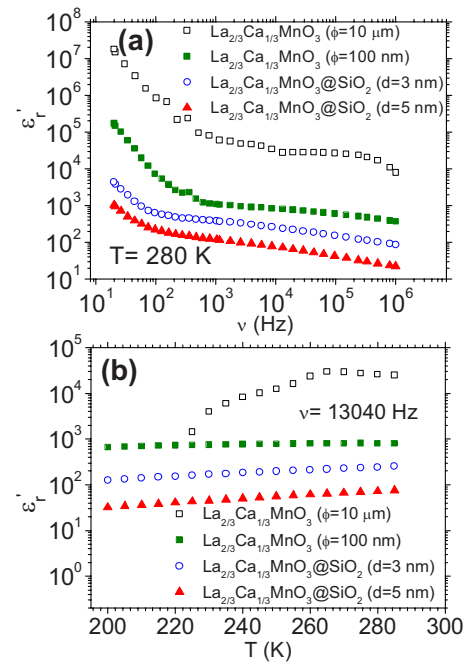


FIG. 1. (Color online) (a) Frequency and (b) temperature dependence of the dielectric constant of the different $\text{La}_{2/3}\text{Ca}_{1/3}\text{MnO}_3$ samples. The core of the composites are the $\text{La}_{2/3}\text{Ca}_{1/3}\text{MnO}_3$ nanoparticles.

the sample that consists of uncoated 100 nm particles, at the same temperature and magnetic field, this effect is considerably strong [20% at 13 kHz and 8% at 150 kHz, as shown in Figs. 3(a) and 3(b)]. For the coated samples the effect is strongly reduced: for the sample with a SiO_2 coating of 3 nm it is around 3% at 3 kHz, as seen in Fig. 3(c), and for the 5 nm coating it is almost negligible in all the temperature interval.

It is worth mentioning that the sign of the magnetocapacitance (positive) is the same as in the bulk material. In the latter, the magnetocapacitive effect is due to its intrinsic phase separation, the same that underlies its well-known magnetoresistance. The result agrees with the prediction of

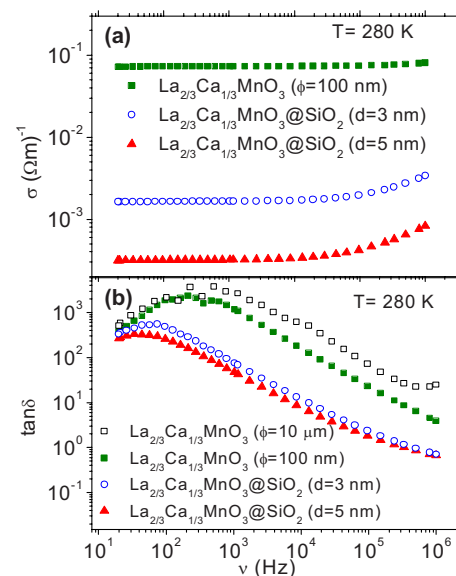


FIG. 2. (Color online) Frequency dependence of (a) the ac conductivity and (b) the loss tangent of the different $\text{La}_{2/3}\text{Ca}_{1/3}\text{MnO}_3$ samples measured at 280 K.

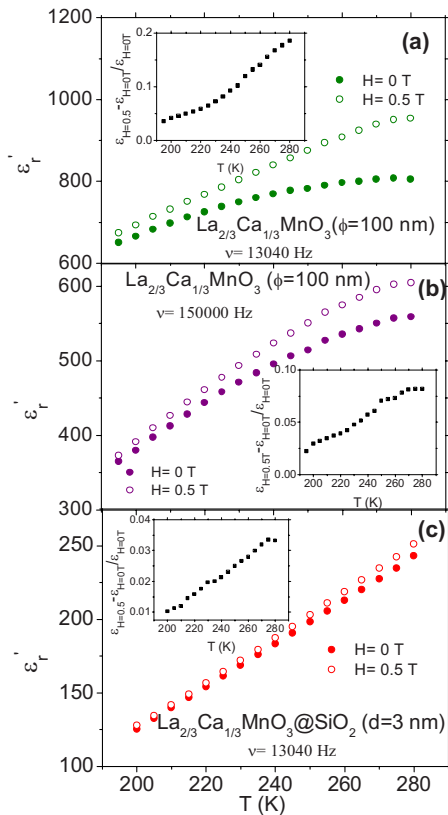


FIG. 3. (Color online) Influence of an external magnetic field on the temperature dependence of the dielectric constant of $\text{La}_{2/3}\text{Ca}_{1/3}\text{MnO}_3$: (a) measured at 13 040 Hz in the $\phi \sim 100$ nm sample, (b) measured at 150 000 Hz in the same sample, and (c) measured in $\text{La}_{2/3}\text{Ca}_{1/3}\text{MnO}_3 @ \text{SiO}_2$ ($d=3$ nm) at 13 040 Hz.

Catalan,¹⁰ who has shown that in the case of core-dominated magnetoresistance the magnetocapacitance will be positive, and negative in interface-dominated magnetoresistance. In the samples presented here, the role of interfaces has been enhanced with the 100 nm particle-size materials, therefore it could be expected a contribution of this extra interfacial term to the global behavior, which could even change the sign of the magnetocapacitance. Nevertheless, from the data of Figs. 3(a) and 3(b) (the sign keeps on being positive) and the impedance diagram of Fig. 4 (that show two arcs: a large arc that is due to the intrinsic response of the material and a second small arc that should have an extrinsic origin) it seems that the role of core effects is still dominating. When lowering temperature, impedance diagrams show that the intrinsic contribution becomes more important and, below 150 K, it is the only one in practice. Added to this we have to note that the shift in the maximum of resistance decreases in temperature with the diminution of the grain size.¹⁵

The results we have shown so far point to a trend that helps in finding a way to a compromise solution. The con-

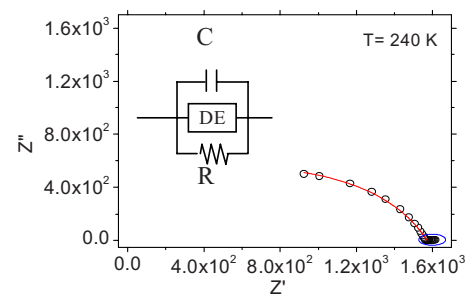


FIG. 4. (Color online) Impedance complex plane diagram of the $\text{La}_{2/3}\text{Ca}_{1/3}\text{MnO}_3$ nanoparticles and its corresponding fit, representative of all the temperature and frequency range studied.

ductivity is decreased, obviously, with the increase in interfaces and coating with SiO_2 and, at the same time, the dielectric constant decreases; weighing both trends with the loss factor, we find that there is compensation. Moreover, this compensation is improved with the coating but when magnetocapacitance data are analyzed, the conclusion is that coating the particles is not a path to follow to improve the figures.

Therefore, this work pins the particle size reduction as the correct way to improve simultaneously the magnetocapacitive properties at room temperature and the dielectric figures of merit of $\text{La}_{2/3}\text{Ca}_{1/3}\text{MnO}_3$, a material where magnetocapacitance is possible without any magnetoelectric coupling.

This work was supported by the Spanish Ministry of Education and Science (MEC) under Project No. FEDER MAT 2007-66696 and by the Xunta de Galicia (XG) under Project No. PGIDIT06PXB103298PR.

¹H. Schmid, *Ferroelectrics* **162**, 317 (1994).

²W. Eerenstein, N. D. Mathur, and J. F. Scott, *Nature (London)* **442**, 759 (2006).

³T. Goto, T. Kimura, G. Lawes, A. P. Ramirez, and Y. Tokura, *Phys. Rev. Lett.* **92**, 257201 (2004).

⁴N. A. Hill and K. M. Rabe, *Phys. Rev. B* **59**, 8759 (1999).

⁵T. Kimura, T. Goto, H. Shintani, K. Ishizaka, T. Arima, and Y. Tokura, *Nature (London)* **426**, 55 (2003).

⁶L. Mitoseriu, D. Marre, A. S. Siri, and P. Nanni, *Appl. Phys. Lett.* **83**, 5509 (2003).

⁷C. Pecharromán, F. Esteban-Bretegón, J. F. Bartolomé, S. López-Esteban, and J. S. Moya, *Adv. Mater.* **13**, 1541 (2001).

⁸J. M. D. Coey, M. Viret, and S. von Molnár, *Adv. Phys.* **48**, 167 (1999).

⁹J. Rivas, J. Mira, B. Rivas-Murias, A. Fondado, J. Dec, W. Kleemann, and M. A. Seánarís-Rodríguez, *Appl. Phys. Lett.* **88**, 242906 (2006).

¹⁰G. Catalan, *Appl. Phys. Lett.* **88**, 102902 (2006).

¹¹M. M. Parish and P. B. Littlewood, *Phys. Rev. Lett.* **101**, 166602 (2008).

¹²C. Vázquez-Vázquez, M. C. Blanco, M. A. López-Quintela, R. D. Sánchez, J. Rivas, and S. B. Oseroff, *J. Mater. Chem.* **8**, 991 (1998).

¹³W. Stöber, A. Fink, and E. J. Bohn, *J. Colloid Interface Sci.* **26**, 62 (1968).

¹⁴J. Ross Macdonald, LEVM version 8.0 Complex Nonlinear Squares Fitting Program, 2003.

¹⁵R. D. Sánchez, J. Rivas, C. Vázquez-Vázquez, A. López-Quintela, M. T. Causa, M. Tovar, and S. Oseroff, *Appl. Phys. Lett.* **68**, 134 (1996).